Electrospray Ionization Tandem Mass Spectrometric Determination of Ligand Binding Energies in Platinum(II) Complexes

Loubna A. Hammad, Gerd Gerdes, and Peter Chen*

Laboratorium für Organische Chemie, ETH Zürich, Zürich, Switzerland

Received October 22, 2004

Energy-resolved collision-induced dissociation (CID) cross sections were measured and deconvoluted to determine ligand binding energies for 2,2,2-trifluoroethanol, water, and acetonitrile to a cationic (diimine)Pt^{II} complex involved in recent C−H activation studies for which ligand exchange is rate-determining. The binding energies agree well with predictions based on DFT calculations. Practical considerations in the use of CID cross sections for large organometallic complexes are discussed. Results using a simplifying approximation for the deconvolution of the binding energy are then introduced and shown to lead to acceptable binding energies when the molecule is large.

Introduction

Mechanistic investigations of C−H activation by homogeneous Pt and Ir complexes had started as model studies[1] for the Shilov reaction[2] and have become testing grounds for new structural types that hold the promise of selective, designed reactivity.[3] Whereas the sensitivity and selectivity of modern in situ spectroscopy, particularly NMR, has greatly facilitated the study of the elementary steps in C−H activation,[4] and kinetics have provided experimental tests of detailed mechanistic proposals,[5,6] a long-standing problem for explanatory or predictive models in C−H activation, in particular, or organometallic chemistry, in general, is the paucity of systematic, reliable thermochemical data for the actual systems under investigation.[7] A variety of thermochemical methods, from reaction calorimetry[8] to photoacoustic methods,[9] for example, have been applied, but the coverage with regard to various structural types is far from being complete. Mass spectrometric methods have been implemented, with some of the more extensive surveys having been done by Rodgers and Armentrout,[10] but the application has not yet come to the fully articulated, large complexes involved in C−H activation or other comparably complicated catalytic reactions due to practical limitations that have made the otherwise suitable technology more difficult to put into routine use for large organometallic systems. We report an electrospray ionization tandem mass spectrometric study of a series of complexes of the general structure **1** with 2,2,2-trifluoroethanol (TFE),[11] water, and acetonitrile as ligands in which the binding energies of the ligands are determined by collision-induced dissociation (CID) appearance curve measurements. While the extraction of thermochemical information from the experimental measurements is done with a procedure well established for small ions,[12] we explore and evaluate simplifications that potentially facilitate the determination of dissociation energies from CID energy-resolved cross sections for large organometallic complexes on a more routine basis.

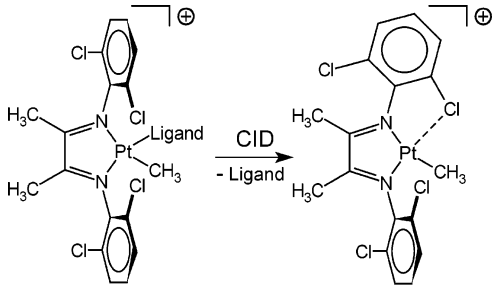

1 (a) Ligand = TFE **2**
(b) Ligand = H_2O
(c) Ligand = CH_3CN

Experimental Section

Preparation of the complexes **1** has been described previously in our earlier mechanistic work on C−H activation.[6] CID

(1) Labinger, J. A.; Bercaw, J. E. *Nature* **2002**, *417*, 507. Stahl, S. S. Labinger, J. A.; Bercaw, J. E. *Angew. Chem., Int. Ed.* **1998**, *37*, 2180. Crabtree, R. H. *Chem. Rev.* **1995**, *95*, 987.

(2) Gol'dschleger, N. F.; Es'kova, V. V.; Shilov, A. E.; Shteinmann, A. A. *Russ. J. Phys. Chem.* **1972**, *46*, 785.

(3) Gerdes, G.; Chen, P. *Organometallics* **2004**, *23*, 3031.

(4) Johansson, L.; Ryan, O. B.; Tilset, M. *J. Am. Chem. Soc.* **1999**, *121*, 1974.

(5) Johansson, L.; Tilset, M.; Labinger, J. A.; Bercaw, J. E. *J. Am. Chem. Soc.* **2000**, *122*, 10846.

(6) Gerdes, G.; Chen, P. *Organometallics* **2003**, *22*, 2217

(7) Marks, T. J. In *Bonding Energetics in Organometallic Compounds*; ACS Symposium Series 428; American Chemical Society: Washington, D.C., 1990; pp 1−17.

(8) Mortimer, C. T. *Rev. Inorg. Chem.* **1984**, *6*, 233.

(9) Klassen, J. K.; Selke, M.; Sorensen, A. A.; Yang, G. K. In *Bonding Energetics in Organometallic Compounds*; ACS Symposium Series 428; American Chemical Society: Washington, D.C., 1990; pp 195−204.

(10) Rodgers, M. T.; Armentrout, P. B. *Mass Spectrom. Rev.* **2000**, *19*, 215. Rodgers, M. T.; Armentrout, P. B. In *Comprehensive Coordination Chemistry II*; McCleverty, J. A., Meyer, T. J., Eds.; Elsevier: Amsterdam, 2004; Vol. 2, pp 141−158.

(11) TFE is a common solvent for a number of C−H activation reactions that use Pt complexes. See refs 3−6.

(12) Armentrout, P. B. *Thermochemical Measurements by Guided Ion Beam Mass Spectrometry*; Greenwich, CT, 1992; Vol. 1. Dalleska, N. F.; Honma K.; Armentrout, P. B. *J. Am. Chem. Soc.* **1993**, *115*, 12125. Khan, F. A.; Clemmer, D. E.; Schultz, R. H.; Armentrout, P. B. *J. Phys. Chem.* **1993**, *97*, 7978. Poutsma, J. C.; Paulino, J. A.; Squires, R. R. *J. Phys. Chem. A* **1997**, *101*, 5336. Rodgers, M. T.; Armentrout, P. B. *J. Phys. Chem. A* **1997**, *101*, 1238. Hammad, L. A.; Wenthold, P. G. *J. Am. Chem. Soc.* **2000**, *122*, 11203. Hammad, L. A.; Wenthold, P. G. *J. Am. Chem. Soc.* **2001**, *123*, 12311.

10.1021/om0491793 CCC: $30.25
Publication on Web 03/16/2005

studies were also reported in that work, although energy-resolved cross-section measurements under single-collision conditions were not performed. For the present study, cationic complexes **1a**−**c** were prepared as 5.5×10^{-5} M solutions by reacting the parent dimethyl complex with HBF_4 in TFE (**1a**), TFE/H_2O (4:1) (**1b**), and TFE/acetonitrile (4:1) (**1c**). Ions **1a**−**c** were transferred to the gas phase by electrospray of their respective solutions into a modified Finnigan MAT TSQ-700 tandem mass spectrometer. Commercial electrospray ionization tandem mass spectrometers are not optimized for energy-resolved cross-section measurements, so there is no guarantee that a suitable kinetic energy distribution for quantitative work can be achieved. A broad distribution of ion energies would seriously impair the extraction of reliable thermochemical information from appearance curves, so modifications in the instrument and in measurement procedures had to be undertaken. Thermalization of electrosprayed ions by multiple collisions with a buffer gas would produce a Gaussian distribution at a defined temperature, but usually at the cost of ion current (due to scattering). Confinement of the ions in a gas-filled radio frequency (rf) ion guide would eliminate scattering losses, but low-order guides, e.g. quadrupoles, hexapoles, and octopoles, have been demonstrated to induce high-energy deviations from the desired Gaussian distribution due to nonadiabaticity.[13] Practically, Gerlich has shown that nonadiabatic effects can be minimized by increasing the order of the multipole.[14] Because the reaction onset is very sensitive to the population of ions in the high-energy tail of the distribution, we built a 24-pole ion guide—the highest order that we could fabricate and build into the TSQ-700—in place of the transfer octopole. Mechanical drawings and a diagram of the device are given in the Supporting Information. The 24-pole rf ion guide, 38 cm in length, can be run with a buffer or reagent gas at pressures up to 100 mTorr for thermalization or reaction without observable degradation of the ion current. No external longitudinal field is applied; ions move through the ion guide because of a weak longitudinal potential induced by the space charge from the continuous beam of incoming ions. In the present work, the principal significance of this modification is the achievement of a well-defined, narrow distribution of the ions' kinetic and, presumably, internal energies. Ions produced by electrospray were thermalized by collisions with 3 mTorr of argon in the multipole and then mass-selected for CID in the first quadrupole of the TSQ-700. The selected ions were then injected into the octopole collision cell, where they underwent CID with the target gas and subsequent mass analysis in the second quadrupole.

For energy-resolved CID, the cross sections for product formation are measured while the octopole rod offset is scanned. The CID cross sections were measured at three different pressures and extrapolated to $p = 0$ to obtain the cross sections under single-collision conditions. The ion energy distribution is considerably narrower when the first quadrupole is operated in "rf only" mode as compared to the more conventional "daughter" mode, so the former mode was used for all measurements in this report. Practically, this means that the quadrupole acts as a high-pass filter rather than a selector for a given mass, but the absence of significant ions at *m/z* higher than **1a**−**c** makes this limitation unproblematic. In the event that higher mass ions were to be present, we have found that difference curves, with the high-pass limit set just above and just below the target mass, provide reliable mass selection without sacrificing the narrow distribution achieved by "rf only" mode. Retarding potential measurements for ions confirms that the modified instrument displays a narrow, Gaussian distribution of ion energies with a full-width half-maximum (fwhm) of 1.51 eV in the laboratory frame, as shown in Figure 1. Absolute cross sections, σ_p, were calculated as described by Ervin et al.[16] using a measured effective path length of 23 ± 5 cm. The uncertainty in the absolute cross sections is estimated to be ±50%.

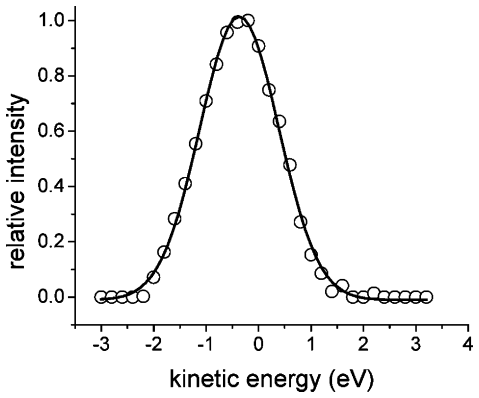

Figure 1. Experimental distribution of ion kinetic energies in the laboratory frame determined by retarding potential measurements after the gas-filled 24-pole ion guide for ion **1c**. The Gaussian fit gives a fwhm of 1.51 eV in the laboratory frame.

Extraction of thermochemical information was performed with the CRUNCH program, version D1,[15,16] which fits the dissociation cross section σ to eq 1:

$$\sigma(E) = \left(\frac{n\sigma_0}{E}\right)\sum_i g_i \int_{E_0-E_i}^{E} [1 - \exp(-k(\epsilon + E_i)\tau)](E - \epsilon)^{n-1}\, d\epsilon \quad (1)$$

where E is the collision energy in the center-of-mass frame, E_0 is the reaction threshold energy at 0 K, σ_0 is a scaling factor, and n is an adjustable parameter. The summation is over i rovibrational states with energies E_i and populations g_i. The latter are assumed to follow a Maxwell−Boltzmann distribution at the temperature of the experiment. The parameter k is the RRKM dissociation rate for the ion with a residence time τ in the collision cell. The parameters σ_0, n, and E_0 are then optimized with a nonlinear least-squares analysis to give the best fit to the data.[23] Equation 1 requires the frequencies for the complexes and transition states (to compute k), which were taken from quantum chemical calculations using Gaussian 98 running on AMD Athlon (Red Hat Linux 7.1) machines.[17] The structures for **1a**−**c**, as well as the dissociation products, were optimized with density functional theory (DFT) using the B3PW91 method with the Stuttgart/Dresden basis set (SDD, which includes an effective core potential for the Pt) for Pt and N,[18] 6-31G** for Cl and O,[19] and 3-21G for C, H, and F.[20] The optimized structures were checked with frequency calculations to verify that they were in fact minima. Single-point energies were then computed at the optimized structures with the same method, but the SDD basis set for Pt and 6-31G** for all other atoms.

The transition state for the dissociation is characterized by the activation entropy, $\Delta S^{\ddagger}$, calculated using eq 2, where $Q^{\ddagger}$ and Q are the partition functions of the transition state and the activated complex, respectively, and $E_{vr}^{\ddagger}$ and E_{vr} are the corresponding average rovibrational energies. By convention, the activation entropy is calculated at 1000 K. Noncovalently bound complexes, such as those employed in this work, are

(13) Anderson, S. G.; Blades, A. T.; Klassen, J.; Kebarle, P. *Int. J. Mass Spectrom. Ion Processes* **1995**, *141*, 217.

(14) Gerlich, D. In *State-Selected and State-to-State Ion−Molecule Reaction Dynamics, Part 1*; Ng, C. Y., Baer, M., Eds.; John Wiley & Sons: New York, 1992; pp 1−176.

(15) CRUNCH, version D1, was kindly provided as an executable by Prof. P. Armentrout.

(16) Ervin, K. M.; Armentrout, P. B. *J. Chem. Phys.* **1985**, *83*, 166. Schultz, R. H.; Crellin, K. C.; Armentrout, P. B. *J. Am. Chem. Soc.* **1991**, *113*, 8590. Dalleska, N. F.; Honma, K.; Sunderlin, L. S.; Armentrout, P. B. *J. Am. Chem. Soc.* **1994**, *116*, 3519.

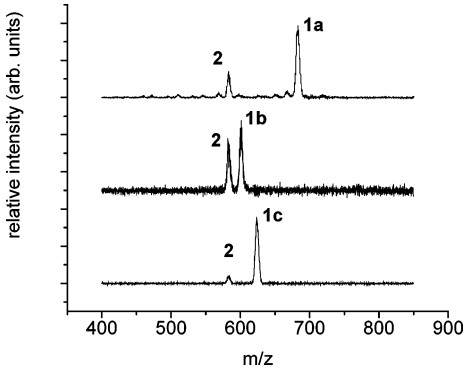

Figure 2. Mass spectra in daughter mode of **1a**−**c** after collision with 0.1 mTorr argon at 40 eV lab. In each case, the simple loss of ligand is the predominant product channel.

expected to proceed through loose transition states and have activation entropies greater than zero.[21]

$$\Delta S^{\ddagger} = k_B \ln Q^{\ddagger}/Q + (E_{vr}{}^{\ddagger} - E_{vr})/T \qquad (2)$$

Results

Ions **1a**−**c** were electrosprayed from their respective solutions, selected by *m/z*, and then subjected to collision-induced dissociation (CID) with argon or xenon target gas. The daughter spectra for the three species are shown in Figure 2. No difference in the CID products were seen when the target gas was changed from argon to xenon. In each case, the ion shows only one significant dissociation channel corresponding to loss of the ligand, which makes complexes **1** ideal for thermochemical determinations using energy-resolved cross-section measurements. The loss of ligand from **1a**−**c** is a simple bond dissociation reaction occurring without a reverse energy barrier.[22] Rodgers et al.[23] have determined that the transition state for simple bond cleavage reactions is best described as a loose orbiting transition state consisting of the dissociation products for which CRUNCH uses a variational transition state model. This "phase space limit" model has been used for fitting a wide variety of energy-resolved cross-section data for larger systems such as the dissociation of alkali metals from crown ethers,[24] the dissociation of transition metal ions from solvent clusters,[25] and the interaction of alkali metal ions with nucleic acid bases.[26] We have therefore used this transition state model for the systems studied in this paper.

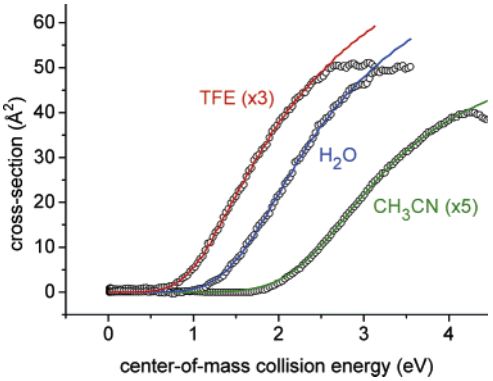

Figure 3. Product cross sections for collision-induced dissociation of **1a**−**c** with Ar target as a function of translational energy in the center-of-mass frame. The experimental data (circles) are the averages of several replicate data sets. The solid line is the model appearance curve calculated using eq 1 convoluted over the neutral and ion kinetic energy distributions, and over RRKM dissociation probabilities.

Of most direct interest are the ligand dissociation energies from Pt^{II} complex **1**, E_0, which can be directly compared to computed values, or checked against solution-phase equilibrium constants. Dissociation energies, E_0, were obtained from energy-resolved collision-induced dissociation (CID) cross sections. The cross sections obtained for formation of TFE, H_2O, and CH_3CN from complexes **1a**−**c** are shown in Figure 3. The apparent energy onsets for the dissociations differ depending on the identity of the ligand. The lowest energy onset is observed for formation of TFE from cationic complex **1a** at ~1 eV, while the onset for acetonitrile formation from complex **1c** is the largest of the three at about 2 eV. The dissociation energies obtained by modeling the CID cross sections using eq 1, along with the corresponding n and $\Delta S^{\ddagger}$, are listed in Table 1, and the fits to the data are shown in Figure 3. The uncertainties on the measured E_0 values include contributions from the standard deviation of the values from replicate measurements, a 0.15 eV (lab) contribution to account for the uncertainty of the energy scale, and an uncertainty due to the choice of the transition state model. The uncertainty in the transition state model corresponds to the effect on the threshold if the activation entropy changed by ± R J/mol K.[27]

The entropies of activation, $\Delta S^{\ddagger}_{1000}$, are also shown in Table 1. As expected, ligand dissociation from complexes **1a**−**c** all have entropies greater than zero, which indicates loose transition states for these reactions. Dissociation of TFE from complex **1a** proceeds through the loosest transition state, as its activation entropy is the highest. The activation entropy for the dissociation of water from complex **1b** is surprisingly low, although its value is still positive. The activation entropy is

(17) Frisch, M. J.; Trucks, G. W.; Schlegel, H. B.; Scuseria, G. E.; Robb, M. A.; Cheeseman, J. R.; Zakrzewski, V. G.; Montgomery, J. A., Jr.; Stratmann, R. E.; Burant, J. C.; Dapprich, S.; Millam, J. M.; Daniels, A. D.; Kudin, K. N.; Strain, M. C.; Farkas, O.; Tomasi, J.; Barone, V.; Cossi, M.; Cammi, R.; Mennucci, B.; Pomelli, C.; Adamo, C.; Clifford, S.; Ochterski, J.; Petersson, G. A.; Ayala, P. Y.; Cui, Q.; Morokuma, K.; Malick, D. K.; Rabuck, A. D.; Raghavachari, K.; Foresman, J. B.; Cioslowski, J.; Ortiz, J. V.; Stefanov, B. B.; Liu, G.; Liashenko, A.; Piskorz, P.; Komaromi, I.; Gomperts, R.; Martin, R. L.; Fox, D. J.; Keith, T.; Al-Laham, M. A.; Peng, C. Y.; Nanayakkara, A.; Gonzalez, C.; Challacombe, M.; Gill, P. M. W.; Johnson, B. G.; Chen, W.; Wong, M. W.; Andres, J. L.; Head-Gordon, M.; Replogle, E. S.; Pople, J. A. *Gaussian 98*, revision A.9; Gaussian, Inc.: Pittsburgh, PA, 1998.
(18) Bergner, A.; Dolg, M.; Kuechle, W.; Stoll, H.; Preuss, H. *Mol. Phys.* **1993**, *80*, 1431. Dolg, M.; Stoll, H.; Preuss, H.; Pitzer, R. M. *J. Phys. Chem.* **1993**, *97*, 5852.
(19) Hariharan, P. C.; Pople, J. A. *Theor. Chim. Acta* **1973**, *28*, 213.
(20) Binkley, J. S.; Pople, J. A.; Hehre, W. J. *J. Am. Chem. Soc.* **1980**, *102*, 939.
(21) Ervin, K. M. *Chem. Rev.* **2001**, *101*, 391.
(22) Nelson, E. D.; Li, R.; Kenttämaa, H. I. *Int. J. Mass Spectrom. Ion Processes* **1999**, *185/186/187*, 91.
(23) Rodgers, M. T.; Ervin, K. M.; Armentrout, P. B. *J. Chem. Phys.* **1997**, *106*, 4499.
(24) More, M. B.; Ray, D.; Armentrout, P. B. *J. Am. Chem. Soc.* **1999**, *121*, 417.
(25) Vitale, G.; Valina, A. B.; Huang, R.; Amunugama, R.; Rodgers, M. T. *J. Phys. Chem. A* **2001**, *105*, 11351.
(26) Rodgers, M. T.; Armentrout, P. B. *J. Am. Chem. Soc.* **2000**, *122*, 8548.
(27) Wenthold, P. G. *J. Phys. Chem. A* **2000**, *104*, 5612.

Table 1. Experimental and Theoretical Thermochemical Data for the Dissociation of Complexes 1a−c

	E_0 (expt, RRKM)					
complex	eV	kcal/mol	kinetic shift, eV	n	$\Delta S^{\ddagger}$, J/mol K	E_0(calc, DFT), kcal/mol
1a	1.19 ± 0.06^a	27.4 ± 1.4^a	1.00	1.3 ± 0.3^a	69	24.3
	1.15 ± 0.06^b	26.5 ± 1.4^b		1.2 ± 0.3^b		
1b	1.26 ± 0.04^a	29.1 ± 0.9^a	1.14	1.1 ± 0.1^a	1	29.3
	1.23 ± 0.04^b	28.4 ± 0.9^b		1.0 ± 0.1^b		
1c	1.52 ± 0.05^a	35.1 ± 1.2^a	1.85	1.0 ± 0.1^a	10	40.5
	1.48 ± 0.05^b	34.1 ± 1.2^b		1.0 ± 0.1^b		

[a] Values obtained from CID with Ar. [b] Values obtained from CID with Xe.

largely determined by the molecular parameters used to model the energized molecule and the transition state. In the phase space limit model employed here, the activation entropy will be very sensitive to the rotational constants of the products as they are assigned to the transitional modes of the transition state.[23] To determine the effect the molecular parameters of the reactant and the transition state have on the dissociation energies and activation entropies, we have refit the curve for complex **1b** in Figure 2 after treating the H_2O torsion in the reactant complex **1b** as a 1-D rotor with a rotational constant of 12 cm^{-1}. This treatment yielded a larger activation entropy, $\Delta S^{\ddagger}_{1000}$, of 19 J/mol K for H_2O loss from complex **1b** but did not effect the calculated dissociation energy, E_0.[25]

The data in Figure 3 were also treated using the loose transition state model.[28] In this model, the vibrational frequencies for the transition state are taken to be the same as those of the products, with the remaining five vibrational frequencies taken from the transitional frequencies for ligand loss of the reactant complex and divided by 10. This treatment also yielded larger activation entropies for ligand loss from complexes **1a**−**c**, but the dissociation energies, E_0, determined for these systems remained unchanged within the reported experimental error.

From solution-phase results, one knows already that the binding of the ligands to the Pt^{II} complexes goes in the qualitative order TFE < $H_2O \ll CH_3CN$; equilibria detected by ^1H NMR find for ligand exchange reactions on complexes very close (structurally) to **1** that $\Delta H^{\circ}_{298} = 3.25 \pm 0.12$ kcal mol^{-1} and $\Delta S^{\circ}_{298} = 2.49 \pm 0.33$ cal mol^{-1} K^{-1} for replacement of water by TFE in wet TFE solution.[29] If one were to assume that there is no large difference between the solvation of water versus TFE in bulk TFE, then the enthalpy and entropy differences would pertain to the relative binding of the two ligands to the Pt^{II} center. The binding of acetonitrile was reported to be so much stronger that equilibrium concentrations of the aqua or TFE complexes could not be detected in the presence of significant amounts of acetonitrile.[30] Nevertheless, our measured difference in binding energies between water and TFE, $\Delta E_0 = 1.6 \pm 1.7$ kcal mol^{-1}, is in satisfactory agreement with the solution-phase results, especially considering that the diimine ligand in **1a**−**c** is close, but not identical, to the one used in solution-phase experiments.[29] Moreover, the solution-phase values contain some (probably small) contribution due to the differing interactions of either water or TFE with the TFE solvent, which should affect both ΔH and ΔS. Comparing the binding energies from the CID appearance curve measurements to the computed values from DFT calculations, we found that, while energies computed with a small basis set err even in the relative order of stability among ligands, a modestly larger basis set gives rather good agreement for the absolute binding energies, providing confidence that the experimental method produces reliable results, at least for the well-behaved system under consideration.

Discussion

The most immediate conclusion one can derive from the data is that CID energy-resolved cross-section measurement, with data analysis using CRUNCH,[16] provides chemically relevant thermochemical information for typical-sized organometallic complexes and real ligands. Given that we have shown that electrospray ionization tandem mass spectrometry applied to organometallic chemistry and homogeneous catalysis is not restricted to stripped-down model complexes, but rather can be used on the actual species in catalytic reactions, one can easily see a variety of applications for CID dissociation energy measurements in important systems. There should be no reason to doubt that such measurements, originally developed for less complicated systems, should not work for the larger ones in principle. There are some instrumental issues to be treated, though, but the present work and its antecedents[31] do show that these methodological hurdles can be surmounted.

One can wonder why "real" organometallic systems are not more commonly addressed by a physical methodology that has such evident utility. An explanation, which requires a closer look at the data reduction method, not only illuminates the basic physical chemistry underlying the method as it is commonly implemented, but also suggests some simplifications that need to be evaluated for their suitability as general, routinely applicable procedures for large molecules.

While it is tempting to simply take the point at which the curve in Figure 3 is observed to rise from baseline as the energy needed to surmount the threshold energy, this gives an overestimate of the actual barrier for the reactions studied here. This overestimate is due to the kinetic shift term being large in these systems and is caused by the finite time available for the energized ion

(28) More, M. B.; Ray, D.; Armentrout, P. B. *J. Phys. Chem A* **1997**, *101*, 4254.

(29) Procelewska, J.; Zahl, A.; van Eldik, R.; Zhong, H. A.; Labinger, J. A.; Bercaw, J. E. *Inorg. Chem.* **2002**, *41*, 2808.

(30) Wik, B. J.; Lersch, M.; Tilset, M *J. Am. Chem. Soc.* **2002**, *124*, 12116.

(31) Hinderling, C.; Feichtinger, D.; Plattner, D. A.; Chen, P. *J. Am. Chem. Soc.* **1997**, *119*, 10793. Kim, Y. M.; Chen, P. *Int. J. Mass Spectrom. Ion Processes* **2000**, *202*, 1.

to undergo reaction. At threshold, a reaction is slow. The residence time of the ions in the instrument before detection, however, is on the order of micro- to milliseconds, so a reaction is not observed until the rate exceeds something on the order of 10^3-10^6 s^{-1}, depending on the instrument and its operating conditions. The additional energy above threshold needed to achieve this rate is called the kinetic shift and has been known to be an important factor, at least qualitatively, since the advent of dissociative photoionization studies in the mass spectrometry community in the 1950s produced data of sufficient quality to assess the effect.[32] In general, the kinetic shift becomes larger when the molecule becomes larger and the bond to be broken becomes stronger. Although there are examples of systems with large kinetic shifts, the typical systems studied using CID show small to moderate effects. For example, dissociations of the complexes of imidazole with K^+ or Li^+ are reported to have kinetic shifts of 0.24 and 1.4 kcal mol^{-1}, respectively,[33] which are small (or even within experimental error bounds) compared to the alkali metal cation binding energies of 26 and 50 kcal mol^{-1}. The larger systems under investigation in the present study show much more prominent effects. For **1a**, **1b**, and **1c**, the kinetic shifts are 23, 26, and 43 kcal mol^{-1} for the respective ligand binding energies of E_0 = 27, 29, and 35 kcal mol^{-1}. In other words, the kinetic shift cannot be neglected for reactions of organometallic complexes in the typical size range encountered in homogeneous catalysis.

Accordingly, CRUNCH implements statistical rate theory, e.g., a RRKM calculation, for the kinetic shift, which in turn requires the frequencies at the starting structure and the transition state so that the respective densities of states can be computed.[16] Within this procedure, there are several well-known issues; the first of which is that the need for frequencies means that the deconvolution of an experimental appearance curve requires a quantum chemical calculation for the whole complex, not a stripped-down model. While such a computation is not a major barrier for small molecules, complexes such as **1a**−**c**, with highly articulated ligands, multiple conformers of comparable stability, and second- or third-row transition metals, present a nontrivial challenge to computational chemistry.[34] Moreover, for systems less well characterized than **1a**−**c** (especially when there is coordinative unsaturation), one is faced with the uncertainty that there may not be a reasonable guarantee that the technically feasible computational methods even produce the correct geometry, in which case one would formally reject the computed frequencies as unsuitable for the CRUNCH procedure.[16] There is furthermore the methodologically ugly fact that a quantum chemical calculation needed to deconvolute the experimental data formally includes the answer to the problem that the experiment is supposed to solve.

We wish to explore a simplification that may substantially ameliorate these problems, namely, the replacement of RRKM theory in the calculation of the kinetic shift with a simplified procedure. In the simplification, the actual frequencies of the molecule are replaced by a single effective frequency in a RRKM calculation. This same assumption, as well as other even more extreme assumptions, is made in quantum RRK (QRRK) theory.[35] Nevertheless, QRRK rates show the same asymptotic behavior as RRKM rates, and QRRK results approximate those from RRKM increasingly well as the molecule gets larger. QRRK has already found extensive application as a substitute for RRKM in the numerical modeling of the kinetics in complex gas-phase reaction systems such as combustion,[36] for which the treatment of pressure effects is closely analogous to the handling of kinetic shifts in the present work. If QRRK, despite the more severe approximations, nevertheless delivers acceptable reaction branching ratios, one can be optimistic that the simplified RKKM treatment may be sufficient to treat the kinetic shift. Perhaps the most convincing evidence that a RRKM variant with an effective frequency is physically realistic is provided by two examples. Bozzelli et al.[37] have shown that heat capacities and densities of states for a variety of molecules can be accurately computed from a sharply reduced set, often only two or three frequencies. More direct is a report by Bierbaum and co-workers.[38] Collision-free, unimolecular dissociation rates for polynuclear aromatic hydrocarbons (PAHs) in highly excited rovibronic states (produced by charge recombination and internal conversion) on the ground electronic surface were modeled by a two-frequency RRKM method. In common with the kinetic shift problem, dissociation must occur in a finite time window set, in this case, by radiative deactivation on the millisecond time scale. The good quantitative agreement with laboratory rates showed that the model could be parametrized for a large range of homologous PAHs.

One can conclude that literature precedent suggests that it is plausible that kinetic shifts would be sufficiently well-treated by a model simpler than full RRKM. Although simplicity is certainly attractive, the main benefit for the present application is that one needs only to know (or more likely, fit) the effective frequency and the number of oscillators to do the simplified RRKM calculation. There is no longer a need to do the full quantum chemical geometry optimization and frequency job for every new species under consideration.

To test the suitability of the simplified RRKM model, at least within a given structural type, we have refit the experimental CID appearance curves, producing the results in Table 2 and Figure 4. The loss of ligand from **1a**−**c** is a simple dissociation, proceeding with no reverse barrier via a very loose orbiting transition state for which CRUNCH uses a variational transition state model.[23] This assumption is used for the simplified calculations as well. Figure 4 shows the comparison between simplified and full RRKM fits as the single effective frequency is varied from 250 to 375 to 500 cm^{-1}.

(32) Chupka, W. A. *J. Chem. Phys.* **1959**, *30*, 191. Stockbauer, R.; Rosenstock, H. M. *Int. J. Mass Spectrom. Ion Phys.* **1978**, *27*, 185.

(33) Rodgers, M. T.; Armentrout, P. B. *Int. J. Mass Spectrom.* **1999**, *185*−*7*, 359.

(34) For example, relativistic effects are large and only approximately treated by effective core potentials. Pyykkö, R. *Chem. Rev*. **1988**, *88*, 563.

(35) Kassel, L. S. *J. Phys. Chem.* **1928**, *32*, 225. Kassel, L. S. *J. Phys. Chem.* **1928**, *32*, 1065.

(36) Westmoreland, P. R.; Howard, J. B.; Longwell, J. P.; Dean, A. M. *AIChE J.* **1986**, *32*, 1971. Dean, A. M.; Bozzelli, J. W.; Ritter, E. R. *Combust. Sci. Eng.* **1991**, *80*, 63.

(37) Bozzelli, J. W.; Chang, A. Y.; Dean, A. M. *Int. J. Chem. Kinet.* **1996**, *29*, 161.

(38) Le Page, V.; Snow, T. P.; Bierbaum, V. M. *Astrophys. J.* **2001**, *132*, 233.

Table 2. Experimental and Theoretical Thermochemical Data for the Dissociation of Complexes 1a−c, Comparing Full RRKM to Effective Frequency Fits[a]

	E_0 (eV)	n	$\Delta S^{\ddagger}_{1000}$ (J/mol K)	χ^2
1a (RRKM, full freq)	1.19 (0.06)	1.3 (0.3)	69 (1)	4.99×10^{-3}
1a ($\nu_{eff} = 250$)	0.87 (0.08)	1.4 (0.5)	132 (1)	7.94×10^{-3}
1a ($\nu_{eff} = 375$)	1.12 (0.04)	1.5 (0.3)	150 (2)	4.69×10^{-3}
1a ($\nu_{eff} = 500$)	1.38 (0.02)	1.2 (0.2)	164 (1)	1.08×10^{-2}
1b (RRKM, full freq)	1.26 (0.04)	1.1 (0.1)	0.8 (1)	3.71×10^{-3}
1b ($\nu_{eff} = 250$)	0.95 (0.06)	1.3 (0.3)	39 (1)	6.26×10^{-3}
1b ($\nu_{eff} = 375$)	1.22 (0.05)	1.2 (0.2)	55 (2)	5.68×10^{-3}
1b ($\nu_{eff} = 500$)	1.38 (0.02)	1.2 (0.3)	67 (2)	6.60×10^{-3}
1c (RRKM, full freq)	1.52 (0.05)	0.9 (0.2)	10 (1)	2.36×10^{-3}
1c ($\nu_{eff} = 250$)	1.31 (0.04)	1.3 (0.1)	95 (1)	3.02×10^{-3}
1c ($\nu_{eff} = 375$)	1.58 (0.06)	1.2 (0.3)	113 (1)	2.92×10^{-3}
1c ($\nu_{eff} = 400$)	1.69 (0.06)	0.9 (0.3)	116 (1)	6.60×10^{-4}
1c ($\nu_{eff} = 500$)	1.75 (0.07)	1.0 (0.3)	126 (1)	2.44×10^{-3}

[a] The numbers in parentheses are the uncertainties calculated as described in the text. χ^2 is calculated from the summed squared deviations of the fit to the experimental data points divided by the number of degrees of freedom.

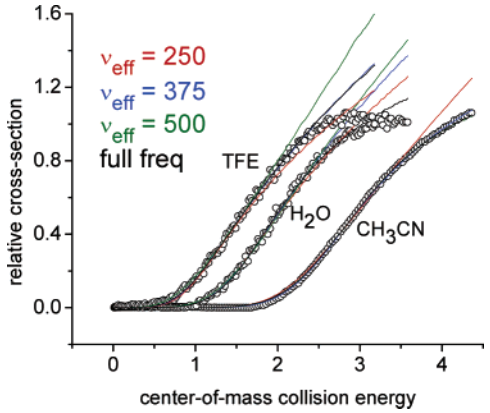

Figure 4. Relative product cross sections for collision-induced dissociation of **1a**−**c** with Ar target as a function of translational energy in the center-of-mass frame. The experimental data (circles) are the averages of several replica data sets. The fit to eq 1 was done using full RRKM (black), or three effective frequencies: 250 cm^{-1} (red), 375 cm^{-1} (blue), or 500 cm^{-1} (green). Some of the fits, for example, black and blue in **1a**, or blue, black, and green in the case of **1c**, overlap.

Interestingly, one sees that the data are all well modeled and that, moreover, an effective frequency of 375 cm^{-1} in the simplified treatment yields a quite satisfactory approximation of the RRKM results. The calculated RRKM dissociation rates for the full frequency set as well as the effective frequencies, 250, 375, and 500 cm^{-1}, are shown in the Supporting Information. It is clear from the comparison that it is possible to choose an effective frequency for each molecule so that the calculated dissociation rate tracks that from the full RRKM calculation over the entire relevant energy range. To be more quantitative, the quality of the fit, as quantified by the χ^2 values over the entire data range, shows that the effective frequency for which the χ^2 is the lowest gives E_0 values that deviate from the full RRKM fits by 0.07, 0.04, and 0.17 eV for **1a**, **1b**, and **1c**, respectively. Moreover, from the χ^2 values, it would be difficult to claim that the full RRKM treatment fits better at all.

Even if one were to take a worst case approach, one can conclude that the sensitivity of the derived dissociation energies E_0 to the effective frequency is quite modest within a given structural class, especially given that the three dissociation energies are rather different and the kinetic shifts are large, ranging from 23 to 42 kcal/mol. Taking the effective frequency from 250 to 500 cm^{-1} results in values for E_0 that vary by only 3−5 kcal/mol, with the full RRKM value always somewhere in the middle of the range. As judged by the χ^2 value for the least well behaved of the three complexes, **1c**, ν_{eff} = 375 and 500 cm^{-1} fit the data about equally well and only slightly less well than full RRKM. A value in between, e.g., $\nu_{eff} = 400$ cm^{-1}, delivers a fit better than any of the others, and even better than the full RRKM. Presumably, a more finely grained search would produce an unambiguous minimum χ^2, but the point made here—that a single ν_{eff} can produce a fit as good as the full RRKM and an E_0 that is not too different—is already shown by the data in Table 2. Although there is clearly more work to be done before one can claim a generally applicable simplification, it appears that an effective frequency close to 375 cm^{-1} gives acceptable values for E_0 for complexes **1** and closely related structures. It should be noted that the effective frequency for structurally different complexes would be expected to be different. A fitting routine for ν_{eff} based on minimizing χ^2 should, in principle, allow the extraction of E_0 without recourse to prior quantum chemical calculations. It should be noted that the relative binding energies, ΔE_0, between TFE, H_2O, and CH_3CN agree well no matter what effective frequency is chosen. This is presumably due to the cancellation of systematic errors in the energy differences.

Conclusion

Ligand dissociation energies from collision-induced dissociation energy-resolved cross-section measurements on Pt^{II} complexes were derived from fitting the appearance curves using a simplified versus the full RRKM model. The results agree well and, moreover, appear to agree well with computed results from DFT. The simplified model does not require a prior quantum chemical calculation of frequencies, indicating that the calculation of the kinetic shift needed in the deconvolution of experimental appearance curves is primarily affected by the number of degrees of freedom with a single effective frequency being derivable from a fit. Methodologically, the simplified model should enable the

extraction of dissociation energies for large molecules, making the CID appearance curve method suitable for the determination of ligand binding energies for large organometallic complexes encountered in catalysis.

Acknowledgment. This work was supported by the Swiss National Science Foundation and the Research Commission of the ETH Zürich. The original construction of the rf 24-pole by Dr. Christian Hinderling is acknowledged.

Supporting Information Available: Computed structures, electronic energies, vibrational frequencies, and rotational constants are provided free of charge via the Internet at http://pubs.acs.org.

OM0491793